

# Comprehensive Modelling of a Capacitor Charger Boost Converter with PID Control

Ilham Agung Wicaksono<sup>1\*</sup>, Lutfir Rahman Aliffianto<sup>2</sup>, Rezki El Arif<sup>3</sup>, Fauzi Imaduddin Adhim<sup>4</sup>

<sup>1,2,3,4</sup> Sepuluh Nopember Institute of Technology, Indonesia

Jl. Teknik Kimia, Keputih, Kec. Sukolilo, Surabaya

<sup>1\*</sup>[Ilham.agung@its.ac.id](mailto:Ilham.agung@its.ac.id), <sup>2</sup>[lrahman@its.ac.id](mailto:lrahman@its.ac.id), <sup>3</sup>[rezki.arif@its.ac.id](mailto:rezki.arif@its.ac.id), <sup>4</sup>[fauzi@eea.its.ac.id](mailto:fauzi@eea.its.ac.id)

## Article history:

Received 25 July 2024  
Revised 15 August 2024  
Accepted 28 August 2024  
Available online 5 September 2024

## Keywords: Boost

Converter,  
Capacitor,  
Transfer Function,  
PID Controller,  
Routh-Hurwitz.

## Abstract

The DC-DC converter is used to convert the DC voltage, and the conversion is carried out to increase or decrease the voltage. This paper discusses the modeling of a boost converter for charging high-capacity capacitors using PID control. PID control is used to overcome changing voltages and long times to steady-state due to capacitor changes. The boost converter has a 24 V input voltage and a 350 V output voltage. Boost converter modeling is performed by electrically reviewing the circuit and then converting the differential equation from the electrical analysis into a state space that depicts the characteristics of boost converter. The simulation was performed using MATLAB software. For the initial conditions, a simulation was carried out using the calculated critical capacitor value to determine whether the boost converter output voltage reached 350 V. Furthermore, when the boost converter was replaced with a 4700  $\mu\text{F}$  capacitor, the boost converter experienced underdamp oscillations with a settling time of up to 9 s. Therefore, PID control was used to overcome oscillations and long settling times. The Ziegler–Nichols 2 and Routh–Hurwitz stability methods were used to determine the parameters  $K_p$ ,  $K_i$ , and  $K_d$ . From the calculation results, the parameters  $K_p = 0.6$ ,  $K_i = 21.39$ , and  $K_d = 0.0042$  are obtained. The output voltage response still has a high undershoot when using the parameters obtained from Ziegler–Nichols 2 tuning, but it already has a fast-settling time. By fine-tuning the PID control, the values  $K_p = 2$ ,  $K_i = 90$ , and  $K_d = 0.09$  were obtained. With these values, the boost converter voltage response has an overshoot of 388 V, an undershoot of 312 V, and a settling time of 0.6 s at 351 V.



This is an open access article distributed under the Creative Commons Attribution License, which permits unrestricted use, distribution, and reproduction in any medium, provided the original work is properly cited. ©2023 by author.

## I. INTRODUCTION

Electrical energy is an energy source that is widely used in everyday life. This use ranges from the household to the industrial scale. Electrical energy produced by generators must have electrical standards that are appropriate to the load; these standards include voltage, frequency, and current. When viewed from voltage standards, two types of voltage that are commonly used: direct voltage (DC) and alternating voltage

<sup>1\*</sup>Corresponding Author

(AC) [1]. The voltage connected to the load must have an appropriate voltage rating for the load. For DC voltage, several voltage levels are commonly used, including 6, 9, 12, 24, and 48 V. This voltage is usually obtained from a battery, accumulator, or AC voltage, which is rectified using a rectifier such as a diode [2].

The load often has different voltage specifications than the source. To obtain a varying DC voltage, a power converter is needed to produce an output voltage according to the required voltage rating. Power converters can generally be divided into two groups depending on the input voltage. If the input voltage is AC voltage, an AC-DC converter is used, which generally uses a rectifier. However, if the input voltage is a DC voltage, then a DC–DC converter is used, which has different voltage specifications from the source. To obtain a varying DC voltage, a power converter is needed that can produce an output voltage according to the required voltage rating. If the input voltage is AC voltage, an AC-DC converter is used, which generally uses a rectifier. However, if the input voltage is DC, a DC–DC converter is used [3], [4]. DC-DC converters can be divided based on the output voltage produced; these converters include buck converters, boost converters and buck-boost converters. Buck converters are used to obtain an output voltage that is lower than the input voltage, and boost converters are used to obtain an output voltage that is higher than the input voltage. Meanwhile, the buck-boost converter can increase and decrease the output voltage level so that the output voltage can be lower or higher than the input voltage [5], [6], [7]. During its development, this DC-DC converter was also used in the field of robotics. Buck converters and buck-boost converters are usually used to reduce battery voltage to supply voltage from the microcontroller [8], whereas boost converters are used to charge capacitors as an energy source in the ball-kicking system on wheeled soccer robots [9], [10], [11].

In this paper, boost converter modeling and simulation are performed to represent the charging of the capacitor used in kicking the ball on the robot. The capacitors chosen to store energy generally have high voltage and capacity specifications so that the energy used to kick the ball can be maximized. There are many approaches to modeling and simulating boost converters, including mathematical, circuit, transfer function, and state space approaches. The approach that is often used is a circuit approach that shows the converter circuit topology on a simulation platform [12]. However, circuit simulation is not fast enough compared with transfer function simulation to describe the ideal conditions of the converter. This ideal condition is useful as literature in the learning process. In addition, this paper will discuss the voltage control of the boost converter. This voltage control is necessary because the voltage from the boost converter will change when the load changes [13]. Voltage control was performed using PID control with Ziegler-Nichols 2 tuning and Routh-Hurwitz stability analysis. Modeling will be performed in MATLAB Simulink without using additional SimPowerSystems or SimElectronic blocksets.

## II. RELATED WORKS

### A. Boost Converter Modelling

Boost converter modeling is performed using a state-space approach. The following is the general form of the state approach written in equations 1 and 2.

$$\dot{x} = Ax + Bu \tag{1}$$

$$y = Cx + Du \tag{2}$$

The boost converter has two conditions, namely ON and OFF, which are representations of switches in the form of transistors or MOSFETs, which are used to regulate the output voltage of the boost converter. From these two conditions, an equation is obtained, which is the state of the boost converter. The boost converter circuit image is shown in Figure 2.1.

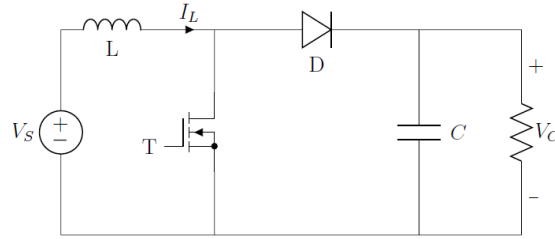


**Figure 1.** Boost Converter Circuit

Next, Figure 2 is presented, which shows the ON condition. This condition occurs when the MOSFET is in a closed condition because the duty cycle is HIGH and the diode is in a reverse biased condition. Therefore, the diode is in the OFF condition. The MOSFET ON condition is described as a connected cable. When in the ON state, in the  $i_L$  loop, the inductor  $L$  will experience charging from the input voltage  $V_S$ , which is denoted by  $U_1$ . The differential equation in this situation is given by equation (3). Furthermore, the  $i_O$  loop is 0 because there is no voltage source. The  $i_O$  loop produces differential equation (4).

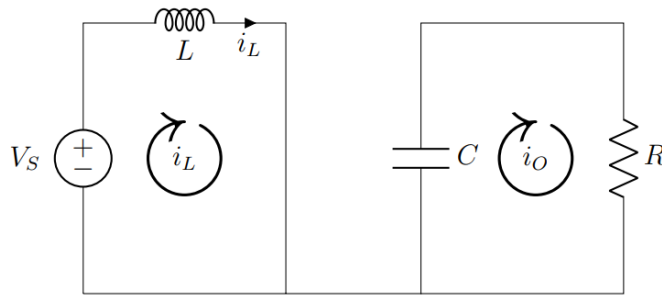


**Figure 2.** Boost Converter ON Condition Circuit Equivalent

$$U_1 = L \frac{di_L}{dt} \quad (3)$$

$$0 = C \frac{dV_C}{dt} + \frac{V_C}{R} \quad (4)$$

Equations (3) and (4) can be rearranged to form equations (5) and (6). We determine that  $V_S = U_1$ ,  $x_1$  is  $i_L$  and  $x_2$  is  $V_C$ . The state space matrices A and B in equation (7) are the equations when the boost converter is in the ON state.

$$\dot{x}_1 = \frac{1}{L} U_1 \quad (5)$$

$$\dot{x}_2 = -\frac{x_2}{RC} \quad (6)$$

$$\begin{bmatrix} \dot{x}_1 \\ \dot{x}_2 \end{bmatrix} = \begin{bmatrix} 0 & 0 \\ 0 & -\frac{1}{RC} \end{bmatrix} \begin{bmatrix} x_1 \\ x_2 \end{bmatrix} + \begin{bmatrix} \frac{1}{L} \\ 0 \end{bmatrix} U_1 \quad (7)$$

When the MOSFET is in the OFF condition, the diode is in the forward bias condition so that it is in the ON condition. The current stored in the inductor in the ON condition will decrease. However, this change in current will be resisted by the inductor by reversing the voltage polarity. Due to the voltage

reversal, the voltage from the source and from the inductor will be connected in series. This voltage will charge the capacitor through the diode, which is in the ON condition. In this condition, the capacitor stores energy from the sum of the source and inductor voltages. The equivalent circuit of the boost converter in the OFF condition is depicted in Figure 3.

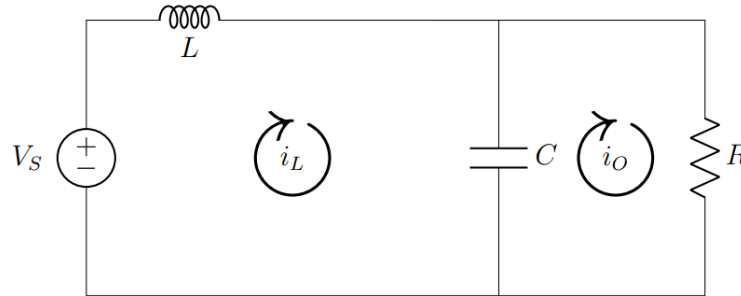


**Figure 3.** Boost Converter OFF Condition Circuit Equivalent

By applying KVL to Figure 3, the state variables are obtained as follows.

$$V_C = u_1 - L \frac{di_L}{dt} \tag{8}$$

$$i_L = C \frac{dV_C}{dt} + \frac{V_C}{R} \tag{9}$$

Equations (8) and (9) can be rearranged to form equations (10) and (11). The state space matrices A and B in equation (12) are the equations when the boost converter is in the OFF state.

$$\dot{x}_1 = -\frac{1}{L} + \frac{1}{L} U_1 \tag{10}$$

$$\dot{x}_2 = \frac{1}{C} x_1 - \frac{1}{RC} x_2 \tag{11}$$

$$\begin{bmatrix} \dot{x}_1 \\ \dot{x}_2 \end{bmatrix} = \begin{bmatrix} 0 & -\frac{1}{L} \\ \frac{1}{C} & -\frac{1}{RC} \end{bmatrix} \begin{bmatrix} x_1 \\ x_2 \end{bmatrix} + \begin{bmatrix} \frac{1}{L} \\ 0 \end{bmatrix} U_1 \tag{12}$$

After deriving the state space matrices A and B for the ON and OFF states of the boost converter, the average of matrices A and B needs to be found by taking into account the duty cycle d [14]. The averages of matrices A and B are shown in equations (14) and (15), respectively.

$$\begin{aligned} \bar{A} &= A_{ON}d + A_{OFF}(1 - d) \\ \bar{A} &= \begin{bmatrix} 0 & 0 \\ 0 & -\frac{1}{RC} \end{bmatrix} d + \begin{bmatrix} 0 & -\frac{1}{L} \\ \frac{1}{C} & -\frac{1}{RC} \end{bmatrix} (1 - d) = \begin{bmatrix} 0 & -\frac{1-d}{L} \\ \frac{1-d}{C} & -\frac{1}{RC} \end{bmatrix} \end{aligned} \tag{13}$$

$$\begin{aligned} \bar{B} &= B_{ON}d + B_{OFF}(1 - d) \\ \bar{B} &= \begin{bmatrix} \frac{1}{L} \\ 0 \end{bmatrix} d + \begin{bmatrix} \frac{1}{L} \\ 0 \end{bmatrix} (1 - d) = \begin{bmatrix} \frac{1}{L} \\ 0 \end{bmatrix} \end{aligned} \tag{14}$$

If equations (13) and (14) are substituted with equation (1), it will produce equation (15).

$$\begin{bmatrix} \dot{x}_1 \\ \dot{x}_2 \end{bmatrix} = \begin{bmatrix} 0 & -(1-d) \\ (1-d) & \frac{1}{RC} \end{bmatrix} \begin{bmatrix} x_1 \\ x_2 \end{bmatrix} + \begin{bmatrix} 1 \\ \frac{1}{L} \\ 0 \end{bmatrix} U_1 \quad (15)$$

Then, to get the output state from  $V_C$  and  $i_L$ , the output state space for matrices C and D is shown in equation (16)

$$\begin{bmatrix} y_1 \\ y_2 \end{bmatrix} = \begin{bmatrix} 1 & 0 \\ 0 & 1 \end{bmatrix} \begin{bmatrix} i_L \\ V_C \end{bmatrix} + \begin{bmatrix} 0 \\ 0 \end{bmatrix} U_1 \quad (16)$$

### B. Capacitor Charging

Previous research carried out the charging process on a supercapacitor using a buck converter. The use of a buck converter is intended to regulate the voltage so that it does not exceed the voltage specifications of the 58 F 20 V

supercapacitor. The charging process was performed using a dedicated LT1074 IC. The charging process reaches the full 20 V condition within 20 s. When the supercapacitor voltage reaches full, the output current from the converter will gradually decrease [15].

### III. METHODS

As can be seen in Figure 1, the boost converter has several components such as MOSFETs, inductors, capacitors, diodes, and resistors. The values of these components must be determined, so that the boost converter has the appropriate output voltage. In this paper, a boost converter is discussed to increase the voltage from 24 V to 350 V. The following is a list of component values and parameters needed for the boost converter.

**Table 1.** 350V Boost Converter Parameters

Parameters	Symbol	Values
Input Voltage	$V_{IN}$	24 V
Output Voltage	$V_{OUT}$	350 V
Frequency	$f$	60 kHz
Input Current	$I_{IN}$	30 A
Voltage Ripple	$\delta$	0.01 V
Duty cycle	$d$	0.9314
Inductor	$L$	0.0012 H
Capacitor	$C$	9.1242 $\mu F$
Output Current	$I_{OUT}$	2.0571 A
Resistor	$R$	170.14 $\Omega$

For the initial conditions, a simulation was performed using the capacitor values according to the calculated values. This condition is performed to determine whether the boost converter has an output of 350 V. When using the capacitor in table 1, the following state-space boost converter is shown in equation (17).

$$\begin{bmatrix} \dot{x}_1 \\ \dot{x}_2 \end{bmatrix} = \begin{bmatrix} 0 & -55.21 \\ 7515 & -644.2 \end{bmatrix} \begin{bmatrix} x_1 \\ x_2 \end{bmatrix} + \begin{bmatrix} 805.2 \\ 0 \end{bmatrix} U_1 \quad (17)$$

If equation (17) is changed to a transfer function, it becomes equation (18) which is the transfer function of the boost converter output voltage.

$$V_{Cap}(s) = \frac{6051000}{s^2 + 644.2s + 415000} \quad (18)$$

Furthermore, the capacitor used must have a high capacity and voltage. The capacitor value was changed to 4700  $\mu F$ , which is the capacitor used in the robot. If the capacitor value is changed to this value, equation (17) can be rewritten as equation (19).

$$\begin{bmatrix} \dot{x}_1 \\ \dot{x}_2 \end{bmatrix} = \begin{bmatrix} 0 & -55.21 \\ 14.59 & -1.251 \end{bmatrix} \begin{bmatrix} x_1 \\ x_2 \end{bmatrix} + \begin{bmatrix} 805.2 \\ 0 \end{bmatrix} U_1 \quad (19)$$

If equation (19) is changed to a transfer function, it will become equation (20) which is the transfer function for the boost converter output voltage.

$$G(s) = \frac{1.175 \cdot 10^4}{s^2 + 1.251s + 805.6} \quad (20)$$

From equation (20), the PID control parameters are calculated using the Ziegler–Nichols 2 tuning and Routh-Hurwitz stability criteria. Figure 3.1 shows a boost converter control block diagram.  $H(s)$  is a voltage divider circuit used to detect changes in the boost converter output voltage. The voltage divider circuit consists of resistors  $R_1 = 150k\Omega$  and  $R_2 = 11k\Omega$ . When using Ziegler Nichols 2, the  $K_d$  and  $K_i$  values must be set to 0 to obtain the  $K_{CR}$  dan  $P_{CR}$  values.

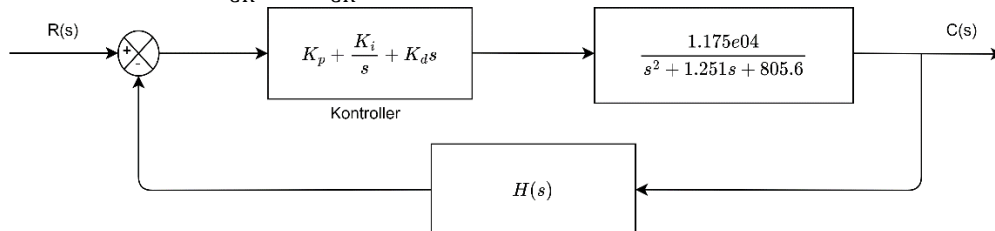


**Figure 4.** Control Block Diagram Boost Converter

With  $(s) = Vs$ ,  $C(s) = V_C$ ,  $K_i = 0$  and  $K_d = 0$ , the following closed-loop transfer function of the boost converter control block diagram is shown in Figure 3.1.

$$\frac{C(s)}{R(s)} = \frac{1.175 \cdot 10^4 \cdot Kp}{(s^2 + 1.251s + (805.6 + 1.175 \cdot 10^4 \cdot Kp)) \cdot H(s)} \quad (20)$$

To obtain the characteristics of an equation, the roots of the denominator of the transfer function equation (20) must be determined.

$$\begin{aligned} (s^2 + 1.251s + (805.6 + 1.175 \cdot 10^4 \cdot Kp)) \cdot H(s) &= 0 \\ s^2 + 1.251s + (805.6 + 1.175 \cdot 10^4 \cdot Kp) &= 0 \end{aligned} \quad (21)$$

The Routh array from equation (21) is as follows.

$s^2$	1	805.6 + 1.175 · 10 <sup>4</sup> · Kp	0
$s^1$	1.251s	0	0
$s^0$	805.6 + 1.175 · 10 <sup>4</sup> · Kp	0	0

By reviewing Routh-Hurwitz stability in a second-order system, the values of  $s^0$ ,  $s^1$  and  $s^2$  must be positive.

$$\begin{aligned}
 805.6 + 1.175 \cdot 10^4 \cdot Kp &> 0 \\
 1.175 \cdot 10^4 \cdot Kp &> -805.6 \\
 Kp &> \frac{-805.6}{1.175 \cdot 10^4} \\
 Kp &> -0.068571429
 \end{aligned} \tag{22}$$

From equation (22) the  $Kp$  value must be more than  $-0.068571429$ . In this condition, the author takes the value  $Kp = 1$ , which is used as the  $Kcr$  value. When  $Kp = 1$ , the characteristic equation (21) will have the following value.

$$s^2 + 1.251s + 12555.6 = 0 \tag{23}$$

To determine the period of continuous oscillation, we substitute  $s = j\omega$  into the characteristic equation (23).

$$\begin{aligned}
 (j\omega)^2 + 1.251(j\omega) + 12555.6 &= 0 \\
 (12555.6 - \omega^2) + 1.251j\omega &= 0 \\
 \omega = 112.5 \vee \omega = 0
 \end{aligned} \tag{24}$$

$Pcr$  is a critical period that causes the system to oscillate periodically. We know that  $\omega = \frac{2\pi}{T}$ , where  $T$  is the period of the wave, which in this situation is  $Pcr$ . From this formula, the  $Pcr$  value can be determined from the  $\omega$  value from equation (24).

$$\begin{aligned}
 \omega &= \frac{2\pi}{Pcr} \\
 Pcr &= \frac{2\pi}{112.51} \\
 Pcr &= 0.0561
 \end{aligned}$$

From the calculations that have been performed, the values obtained are  $Kcr = 1$  dan  $Pcr = 0.0561$ . Next, the values of  $Kp$ ,  $Ki$  and  $Kd$  can be calculated by referring to the Ziegler Nichols 2 table.

$$\begin{aligned}
 Kp &= 0.6 \cdot Kcr \\
 &= 0.6 \cdot 1 \\
 &= 0.6 \\
 Ti &= 0.5 \cdot Pcr \\
 &= 0.5 \cdot 0.0561 \\
 &= 0.02805 \\
 Td &= 0.125 \cdot Pcr \\
 &= 0.125 \cdot 0.0561 \\
 &= 0.0070125
 \end{aligned} \tag{25}$$

With the calculations performed in equation (25), the values  $Kp = 0.6$ ,  $Ki = 21.39$  dan  $Kd = 0.0042075$  were obtained. Next, the PID parameter values were applied to the plant boost converter.

#### IV. RESULTS AND DISCUSSIONS

The capacitor value will be adjusted to table 1, this aims to determine whether the boost converter can reach a voltage of 350 V, along with the output voltage response with the capacitor value according to table 1.

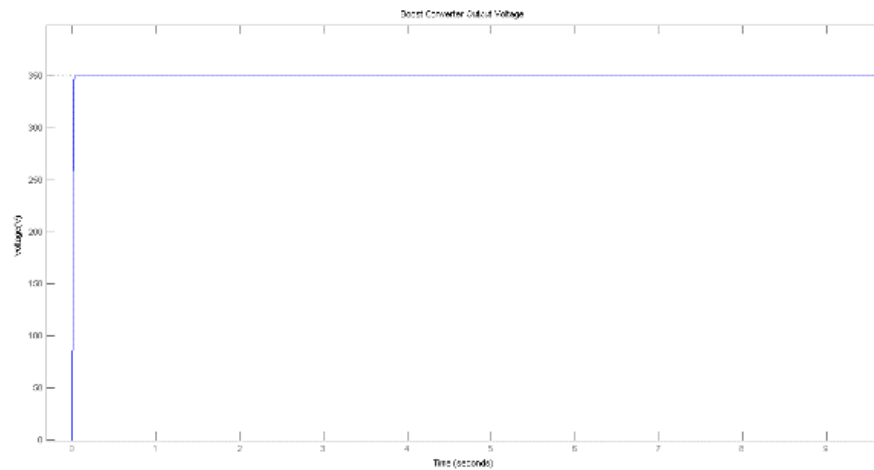


**Figure 5.** Boost Converter Output Voltage without Capacitor Change

Figure 5 shows the output voltage response of the boost converter without changing the capacitor value. The boost converter does not experience overshoot and can achieve settling time within 0.03 s. Next, the boost converter capacitor is replaced with a value of  $4700 \mu F$  without using feedback.

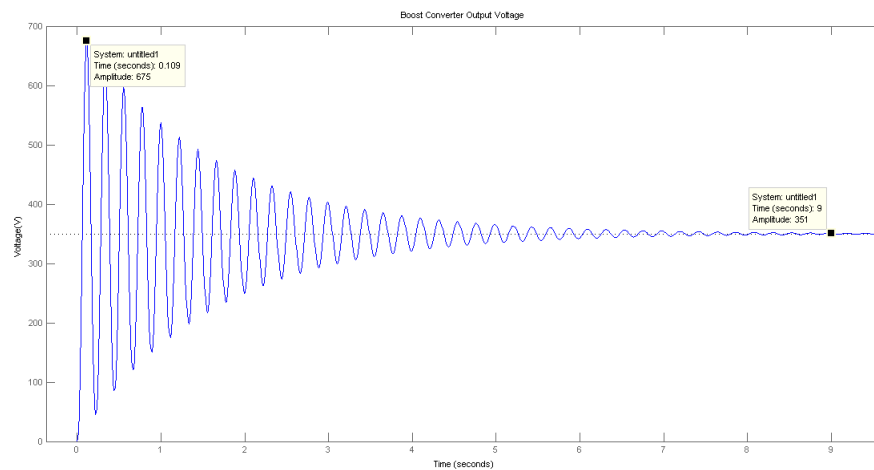


**Figure 6.** Boost Converter Output Voltage without Capacitor Change

After the capacitor value is changed, it can be seen in Figure 6 that the boost converter experiences underdamped oscillations with a maximum overshoot of 675 V and a settling time of 9 s. With high overshoot and a long settling time, changing the capacitor will also take longer. Therefore, PID control is used to reduce overshoot and speed up the settling time of the boost converter so that capacitor charging is



faster. The following is the voltage response of the boost converter using PID control with the Ziegler Nichols 2 tuning parameters, equation (25).

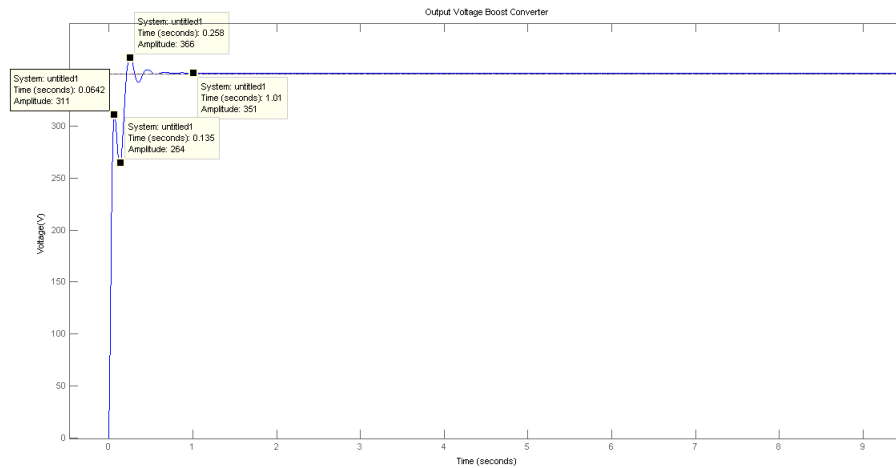


**Figure 7.** Boost Converter Output Voltage Response with PID Control

Figure 7 shows the boost converter response using the Ziegler–Nichols 2 tuning PID control. With PID control, the boost converter voltage experiences an undershoot at 264 V and an overshoot at 366 V. For settling time, the boost converter can stabilize at a voltage of 351 V in 1.01 s. With PID control, the settling time of the boost converter increases. However, the Boost converter still experiences undershoot below 300 V. Therefore, fine tuning was performed again on the PID control parameters.

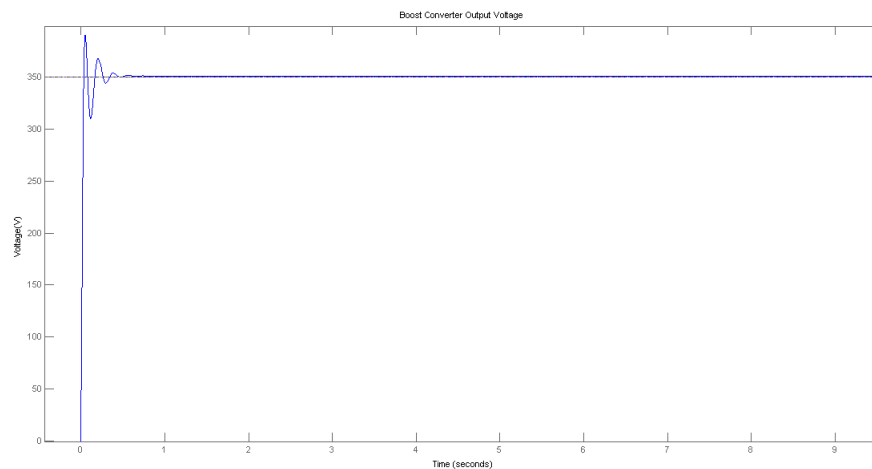


**Figure 8.** Boost Converter Output Voltage Response with Fine Tuning PID Control

Figure 8 shows the boost converter voltage response with parameters  $K_p = 2$ ,  $K_i = 90$  dan  $K_d = 0.09$ . With these parameters, the boost converter has an overshoot of 388V, an undershoot of 312V and a settling time of 0.6s at a voltage of 351 V. With this fine tuning, the previous undershoot can be reduced by 48 V and the settling time is 0.4 s faster. Therefore, for the 4700  $\mu F$  capacitor, PID control parameters

are used from the results of fine tuning so that the charging of the capacitor is faster. Next, the PID control parameters from the fine-tuning results are tested using several large capacity capacitors.

**Table 2.** Boost Converter Voltage Test Results on Capacitor Changes

Capacitor Value( $\mu F$ )	Overshoot(V)	Undershoot(V)	Settling Time(s)
1500	359	307	0.464
2200	359	313	0.436
2700	360	318	0.454
3300	366	319	0.454
5600	407	302	0.802
6800	424	281	1.17
7500	438	270	1.5
8200	447	257	1.97
9100	461	239	3.53

From the capacitor test results in table 2, as the capacitor capacity value increases, the overshoot value will increase. Meanwhile, the undershoot value of the boost converter output voltage decreases. Therefore, as the capacitor value increases, the underdamped oscillation will take longer. This is proven by the settling time value of the capacitor output voltage, which increases with the capacitor capacity value.

## V. CONCLUSIONS AND RECOMMENDATIONS

PID control can reduce the overdamped oscillation time of the boost converter voltage response if there is a change in the capacitor value. With parameters  $Kp = 2$ ,  $Ki = 90$  and  $Kd = 0.09$ , a 350V boost converter with a  $4700\mu F$  capacitor can achieve a settling time of 0.6s. Furthermore, along with increasing the capacitor capacity value, it is recommended to use a more adaptive controller to reduce underdamped oscillations so that the oscillations decrease, and the output voltage response can achieve steady-state faster.

## VI. REFERENCES

- [1] M. Y. Aswardi and D. T. Yanto, "Teknik elektronika daya," *Indonesia: IRDH Book Publisher*, 2020.
- [2] E. Prianto, N. Yuniarti, and D. C. Nugroho, "Boost-converter sebagai alat pengisian baterai pada sepeda listrik secara otomatis," *Jurnal Edukasi Elektro*, vol. 4, no. 1, pp. 52–62, 2020.
- [3] M. Yuhendri, M. Muskhair, and others, "Optimum Torque Control of Stand Alone Wind Turbine Generator System Fed Single Phase Boost Inverter," in *2018 2nd International Conference on Electrical Engineering and Informatics (Icon EEI)*, 2018, pp. 148–153.
- [4] C. Ibrahim, T. Sukmadi, and A. Nugroho, "Perancangan Pengontrolan Motor DC Menggunakan DC–DC Konverter Class C Mode Motoring dan Regenerative Breaking Untuk Simulasi Kendaraan Listrik," *Transient: Jurnal Ilmiah Teknik Elektro*, vol. 5, no. 3, pp. 338–344, 2017.
- [5] N. Rana, M. Kumar, A. Ghosh, and S. Banerjee, "A novel interleaved tri-state boost converter with lower ripple and improved dynamic response," *IEEE Transactions on Industrial Electronics*, vol. 65, no. 7, pp. 5456–5465, 2017.
- [6] V. C. Peeyush, "Design and Implementation of Boost Converter for IoT Application," *power*, vol. 6, no. 6, 2017.
- [7] M. Cucuzzella, R. Lazzari, S. Trip, S. Rosti, C. Sandroni, and A. Ferrara, "Sliding mode voltage control of boost converters in DC microgrids," *Control Eng Pract*, vol. 73, pp. 161–170, Apr. 2018, doi: 10.1016/j.conengprac.2018.01.009.

- [8] M. Sanggola, C. Mamahit, and F. Seke, "Pengembangan Sistem Gerak Robot Berkaki Enam," *JURNAL EDUNITRO Jurnal Pendidikan Teknik Elektro*, vol. 2, no. 1, pp. 53–60, 2022.
- [9] S. SUSILO, "OPTIMASI CHARGING BOOST KONVERTER DENGAN DUAL OUTPUT PADA ROBOT SEPAKBOLA BERODA," Universitas Islam Sultan Agung, 2019.
- [10] A. Syamsudin, I. K. Wibowo, and M. M. Bachtiar, "Improving The Accuracy and Controlling The Shooting Power in a Wheeled Soccer Robot," in *2018 International Electronics Symposium on Engineering Technology and Applications (IES-ETA)*, 2018, pp. 100–106.
- [11] F. A. Widodo and K. Mutijarsa, "Design and implementation of movement, dribbler and kicker for wheeled soccer robot," in *2017 International Conference on Information Technology Systems and Innovation (ICITSI)*, 2017, pp. 200–205.
- [12] R. H. G. Tan and M. Y. W. Teow, "A comprehensive modeling, simulation and computational implementation of buck converter using MATLAB/Simulink," in *2014 IEEE Conference on Energy Conversion (CENCON)*, 2014, pp. 37–42.
- [13] M. Jamlay and W. M. Faizal, "Dual feedback control dc-dc boost converter menggunakan pi controller," *INOVTEK POLBENG*, vol. 4, no. 2, pp. 91–97, 2014.
- [14] R. H. G. Tan and L. Y. H. Hoo, "DC-DC converter modeling and simulation using state space approach," in *2015 IEEE Conference on Energy Conversion (CENCON)*, 2015, pp. 42–47.
- [15] T. Hranov, G. Vacheva, N. Hinov, and D. Arnaudov, "Modeling DC-DC converter for charging supercapacitors," in *2017 40th International Spring Seminar on Electronics Technology (ISSE)*, 2017, pp. 1–5.